



GEOLOGY OF THE INTERMOUNTAIN WEST

an open-access journal of the Utah Geological Association

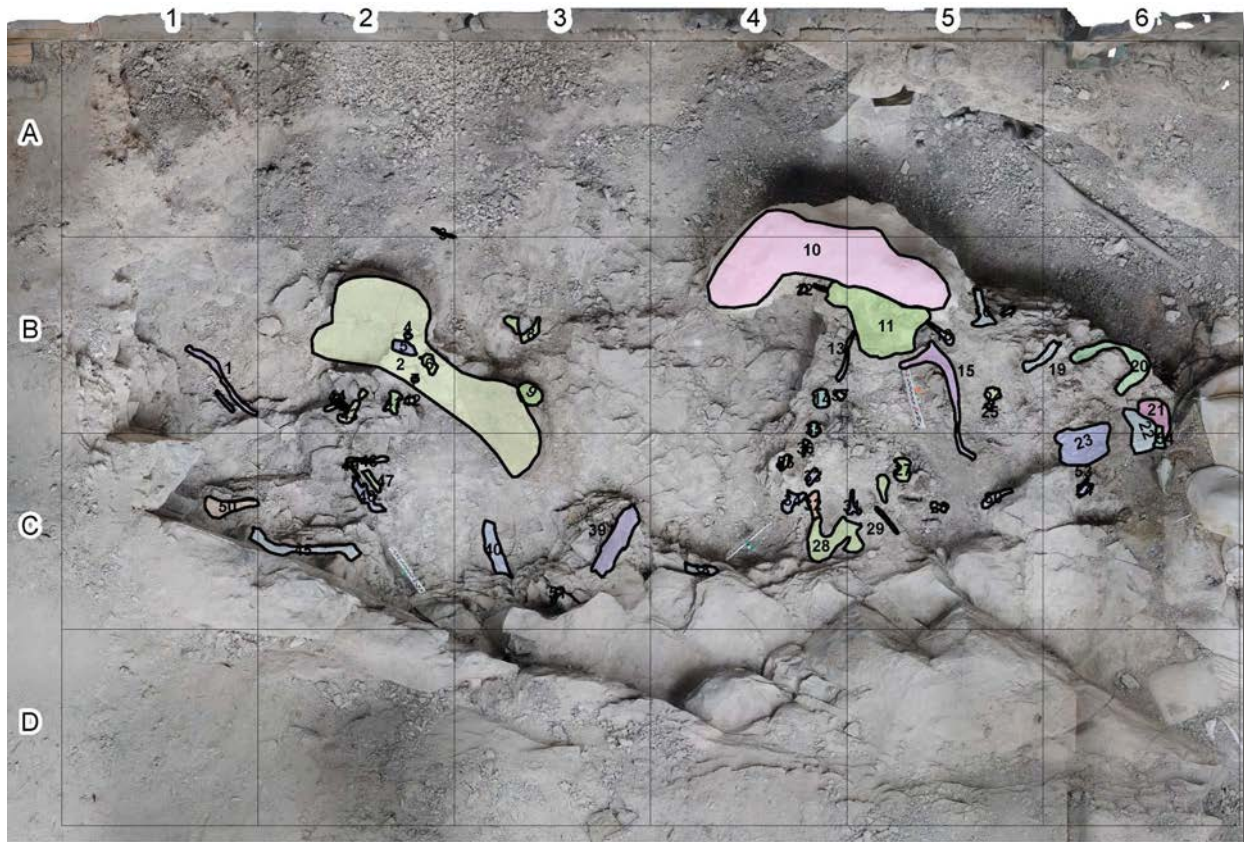
ISSN 2380-7601

Volume 5

2018

CLOSE-RANGE PHOTOGRAMMETRY OF THE CLEVELAND-LLOYD DINOSAUR QUARRY, UPPER JURASSIC MORRISON FORMATION, EMERY COUNTY, UTAH

Jonathan P. Warnock, Joseph E. Peterson, Steven R. Clawson, Neffra A. Matthews, and Brent H. Breithaupt



Theme Issue

An Ecosystem We Thought We Knew—
The Emerging Complexities of the Morrison Formation
SOCIETY OF VERTEBRATE PALEONTOLOGY

Annual Meeting, October 26 – 29, 2016

Grand America Hotel

Salt Lake City, Utah, USA



© 2018 Utah Geological Association. All rights reserved.

For permission to copy and distribute, see the following page or visit the UGA website at www.utahgeology.org for information.

Email inquiries to GIW@utahgeology.org.



GEOLOGY OF THE INTERMOUNTAIN WEST

an open-access journal of the Utah Geological Association

ISSN 2380-7601

Volume 5

2018

Editors

Douglas A. Sprinkel Utah Geological Survey 801.391.1977 GIW@utahgeology.org	Thomas C. Chidsey, Jr. Utah Geological Survey 801.537.3364 tomchidsey@utah.gov
--	---

Bart J. Kowallis Brigham Young University 801.422.2467 bkowallis@gmail.com	Steven Schamel GeoX Consulting, Inc. 801.583-1146 geox-slc@comcast.net
---	---



Society of Vertebrate Paleontology

Editors

Kelli C. Trujillo — University of Wyoming
John Foster — Utah Field House of Natural History
State Park Museum
Cary Woodruff — University of Toronto
Octavio Mateus — Universidade Nova de Lisboa

Production

Cover Design and Desktop Publishing
Douglas A. Sprinkel

Cover

Orthomosaic map of the 2015–2017 excavations of the South Butler Building at the Cleveland-Lloyd Dinosaur Quarry produced from photogrammetry and standard grid mapping. The Cleveland-Lloyd Dinosaur Quarry is located on the San Rafael Swell, Emery County, Utah.



This is an open-access article in which the Utah Geological Association permits unrestricted use, distribution, and reproduction of text and figures that are not noted as copyrighted, provided the original author and source are credited.

UGA Board

October 2018 – September 2019

President	Peter Nielsen	peternielsen@utah.gov	801.537.3359
President-Elect	Leslie Heppler	lheppler@utah.gov	801.538.5257
Program Chair	Gregory Schlenker	gcsgeoscience@gmail.com	801.745.0262
Treasurer	Dave Garbrecht	garbrechtd@yahoo.com	801.916.1911
Secretary	George Condrat	gcondrat@loughlinwater.com	435.649.4005
Past President	Paul Inkenbrandt	paulinkenbrandt@utah.gov	801.537.3361

UGA Committees

Environmental Affairs	Craig Eaton	eaton@ihi-env.com	801.633.9396
Geologic Road Sign	Terry Massoth	twmassoth@hotmail.com	801.541.6258
Historian	Paul Anderson	paul@pbageo.com	801.364.6613
Outreach	Greg Nielson	gnielson@weber.edu	801.626.6394
Membership	Rick Ford	rford@weber.edu	801.626.6942
Public Education	Paul Jewell	pwjewell@mines.utah.edu	801.581.6636
	Matt Affolter	gfl247@yahoo.com	
Publications	Paul Inkenbrandt	paulinkenbrandt@utah.gov	801.537.3361
Publicity	Paul Inkenbrandt	paulinkenbrandt@utah.gov	801.537.3361
Social/Recreation	Roger Bon	rogerbon@xmission.com	801.942.0533

AAPG House of Delegates

2017–2020 Term	Tom Chidsey	tomchidsey@utah.gov	801.537.3364
----------------	-------------	---------------------	--------------

State Mapping Advisory Committee

UGA Representative	Jason Blake	blake-j@comcast.net	435.658.3423
--------------------	-------------	---------------------	--------------

Earthquake Safety Committee

Chair	Grant Willis	gwillis@utah.gov	801.537.3355
-------	--------------	------------------	--------------

UGA Website

www.utahgeology.org

Webmasters	Paul Inkenbrandt	paulinkenbrandt@utah.gov	801.537.3361
------------	------------------	--------------------------	--------------

UGA Newsletter

Newsletter Editor	Bill Lund	uga.newsletter@gmail.com	435.590.1338
-------------------	-----------	--------------------------	--------------

Become a member of the UGA to help support the work of the Association and receive notices for monthly meetings, annual field conferences, and new publications. Annual membership is \$20 and annual student membership is only \$5. Visit the UGA website at www.utahgeology.org for information and membership application.

The UGA board is elected annually by a voting process through UGA members. However, the UGA is a volunteer-driven organization, and we welcome your voluntary service. If you would like to participate please contact the current president or committee member corresponding with the area in which you would like to volunteer.



Close-Range Photogrammetry of the Cleveland-Lloyd Dinosaur Quarry, Upper Jurassic Morrison Formation, Emery County, Utah

Jonathan P. Warnock^{1*}, Joseph E. Peterson², Steven R. Clawson³, Neffra A. Matthews⁴, and Brent H. Breithaupt⁵

¹Indiana University of Pennsylvania, Department of Geoscience, 302 East Walk, Indiana, PA 15705; jwarnock@iup.edu

²University of Wisconsin-Oshkosh, Department of Geology, 800 Algoma Blvd, Oshkosh, WI 54901; petersoj@uwosh.edu

³3315 Cascade Ln., New Lenox, IL 60451; srlawson@comcast.net

⁴Bureau of Land Management National Operations Center, Geospatial Section, Denver Federal Center, Bldg. 50, P.O. Box 25047, OC-534, Denver, CO 80225-0047; n1matthe@blm.gov

⁵Bureau of Land Management, Wyoming State Office, 5353 Yellowstone Road, Cheyenne, WY 82009; bbreitha@blm.gov

*Corresponding Author

ABSTRACT

Bone distribution data are essential for taphonomic assessments of bonebeds. The Cleveland-Lloyd Dinosaur Quarry (CLDQ), an *Allosaurus*-dominated bonebed within the Upper Jurassic Morrison Formation, has been researched for nearly 100 years, but published maps are scarce considering the importance and density of the assemblage. Additionally, few detailed maps of bones from the CLDQ have been published in two dimensions, whereas the third, the stratigraphic/vertical, dimension has never been recorded. Utilizing standard field mapping techniques as well as photogrammetry, the three-dimensional orientations of bones currently exposed in the quarry have been analyzed for potential dispersal patterns. Additionally, a “living” or continuously updatable, photogrammetric map which allows for researchers to view the bones in three dimensions throughout the course of excavation has been created. Continued photogrammetry in future field seasons will allow visualization of bones in three dimensions even after the currently exposed bones have been removed. Utilizing these newly available data, two distinct clusters of bone within the South Butler Building at the quarry are identified. Based on statistically significant average orientations and depths of these bones, early-stage post-mortem transport of carcasses prior to disarticulation (i.e., bloat and float) is supported as an important transport and depositional process within the quarry assemblage. Furthermore, possible evidence of multiple depositional events is discussed.

INTRODUCTION

Upper Jurassic bonebeds of the Morrison Formation are typically sauropod-dominated, with theropods being comparatively rare (Engelmann and others, 2004). Whereas the dominance of sauropods is possibly a re-

lection of Late Jurassic ecosystems (Dodson and others, 1980), low predator:prey ratios may also represent taphonomic bias resulting from pre-burial depositional winnowing and weathering of the more easily-transportable and easily weathered theropod bone elements (Voorhies, 1969; Behrensmeyer, 1975; Gates, 2005).

Citation for this article.

Warnock, J.P., Peterson, J.E., Clawson, S.R., Matthews, N.A., and Breithaupt, B.H., 2018, Close-range photogrammetry of the Cleveland-Lloyd Dinosaur Quarry, Upper Jurassic Morrison Formation, Emery County, Utah: *Geology of the Intermountain West*, v. 5, p. 271–285.

© 2018 Utah Geological Association. All rights reserved.

For permission to use, copy, or distribute see the preceding page or the UGA website, www.utahgeology.org, for information. Email inquiries to GIW@utahgeology.org.

One notable exception, with a predator:prey ratio of 3:1, is the Cleveland-Lloyd Dinosaur Quarry (CLDQ) on the north end of the San Rafael Swell, Emery County, east-central Utah (figure 1), a macrofossil bonebed comprised primarily of the predatory theropod, *Allosaurus fragilis* (Miller and others, 1996). The bonebed is also unusual in that the large number of *Allosaurus* preserved at the quarry (n = 46) are dominated by subadult individuals (Madsen, 1976).

As a result of the distinctly high predator:prey ratio, the CLDQ has frequently been treated as an anomaly and mystery in the literature (e.g., Madsen, 1976; Bilbey, 1999; Gates, 2005; Hunt and others, 2006). A robust taphonomic interpretation of the bonebed is needed in order to understand the CLDQ in relation to Jurassic paleoecology of the region. Additionally, the subadult:adult ratio at the CLDQ cannot be fully interpreted further without development of the quarry's taphonomic model. Understanding whether subadults were more common than adults within the paleogeographic region, or preferentially deposited at the CLDQ for another reason, requires a detailed understanding of the processes which lead to the deposition of the bonebed.

Many competing taphonomic hypotheses have been put forth regarding the CLDQ. Early hypotheses focused on a predator trap, where a few dying herbivores attracted large numbers of carnivores (Dodson and others, 1980; Stokes, 1985; Richmond and Morris, 1996), even though expected taphonomic evidence (i.e., gnaw marks and trampling of bone) to support these conclusions is not present at the site (Gates, 2005). Bilbey (1999) suggested the deposit represents a lethal spring or seep; however, no source of toxin is suggested. Furthermore, it is unlikely that dinosaurs would have been poisoned to the extent that they would have died at the site of the seep upon drinking. Other authors (e.g., Gates, 2005) have evoked a drought-induced assemblage. While the surface textures of most of the recovered bones do not suggest post-mortem subaerial exposure in a dry environment, the presence of abundant, small parautochthonous bone fragments dispersed throughout the quarry matrix suggests that subaerial exposure and intense weathering of some bones was occurring (Gates, 2005; Peterson and others, 2017). Peter-



Figure 1. The Cleveland-Lloyd Dinosaur Quarry (CLDQ) is located in east-central Utah about 185 km (115 mi) southeast of Salt Lake City, Utah.

son and others (2017) utilized novel intramatrix bone fragment (IBF) data and geochemical profiling of bones and sediment in an attempt to synthesize and understand these competing hypotheses. Their data suggest that the deposit represents periods of aridity, leading to the generation of IBF's, followed by one or more flood periods in which the IBF's were incorporated with sediment and dinosaur carcasses, creating a hypereutrophic ephemeral pond. This hypothesis incorporates components of drought and 'bloat and float' deposition as well as flooding (Peterson and others, 2017). A key piece of taphonomic data is missing from all these studies and hypotheses however: three-dimensional (3D) bone distribution.

Despite a great diversity of studies that use the CLDQ as the primary site of study (e.g., Stokes, 1945;

Bilbey; 1999, Hanna, 2002; Suarez, 2003; Gates, 2005; Hunt and others, 2006; Carpenter, 2010; Peterson and others, 2017), maps representing previously excavated bones contain some anomalous gaps (Stokes, 1985), and a lack of 3D distribution of bones. The scope of many studies conducted throughout the 20th century (e.g., Gilmore, 1920; Stokes, 1945; Madsen, 1976) focused on the collection of impressive museum specimens and placed little emphasis on mapping, leaving modern studies at risk of falling prey to cartographic artifacts (Stokes, 1985). Notably, the CLDQ was unprotected and worked by amateur collectors over the period of time spanning the professional collection of bones by Princeton University in 1939 and the University of Utah in 1960 (Madsen, 1976). Due to a lack of cooperation in compiling data, composite maps of the bonebed, including a popularly cited map drafted by the University of Utah Cooperative Dinosaur Project in 1967, offer only general two-dimensional (2D) estimations of the original spatial distribution of bone, and lack any description of stratigraphic position or plunge of bones. Additionally, the available composite map of the quarry contains many numerous artifacts, including artificial right angles at the edges of the bonebed and gaps within bone deposition. In order to understand the depositional history of the quarry, as well as being able to determine whether or not the *Allosaurus* bones were deposited during a single or multiple events, 3D bone orientation data is needed.

In order to address these issues, grid maps composed of previously and recently exposed bones have been drafted over the 2015–2017 field seasons. These maps include depth data relative to a fixed arbitrary datum within the South Butler Building at the quarry as well as depth relative to the undulatory surface of the freshwater limestone cap, which overlies the productive siltstone bonebed for which the site is famous. Finally, we present a “living” photogrammetric map of the quarry which contains 3D bone orientation data. The map is referred to as living because new data, in the form of photographs from future excavations as well as positions of newly exposed bones, can be added to the current file.

Digital photogrammetry, or the process of three-dimensionally reconstructing the surface texture and to-

pography of objects using oriented digital photographs, offers a modern, precise means of resolving the relative positions of bone (Matthews, 2008), and has already seen some applications in the field of vertebrate paleontology (see Breithaupt and others, 2004; Falkingham, 2012; Matthews and others, 2016; and references therein). In the present study, a high-fidelity 3D photogrammetric data file produced for the CLDQ over the course of three field seasons provides a more accurate representation of the quarry assemblage than previously published maps.

GEOLOGICAL SETTING, TAPHONOMY, AND HISTORY OF THE CLEVELAND- LLOYD DINOSAUR QUARRY

The CLDQ is located approximately 38 m above the basal contact of the Brushy Basin Member of the Morrison Formation (Bilbey, 1992; Peterson and others, 2017). The numerous dinosaur fossils in the quarry are encased in a structureless calcareous mudstone composed primarily of montmorillonite with various silicate minerals (e.g., quartz, feldspar, and biotite). The bonebed ranges in thickness from centimeters to approximately 1 meter. The silty calcareous mudstone is overlain by a bone-bearing micritic limestone unit that varies in thickness from 0.3 to 1.0 m (Bilbey, 1992; Gates, 2005). The limestone contains notably fewer bones than the silty mudstone. Based on limited exposures, the silty mudstone unit is laterally continuous for 50 to 75 m before pinching out to the south (Gates, 2005).

A total of ten dinosaur genre are present at the quarry including two ornithischian taxa (*Stegosaurus* and *Camptosaurus*), three sauropod taxa (*Camarasaurus*, *Barosaurus*, and *Apatosaurus*), and five theropod taxa (*Allosaurus*, *Ceratosaurus*, *Stokesosaurus*, *Marshosaurus*, and *Torvosaurus*) (Gates, 2005; Foster and Peterson, 2016). Of all the present taxa, *Allosaurus fragilis* is the most abundant (46 skeletons) composing 66% of the total skeletons (Gates, 2005).

Due to its abnormal abundance of large theropod dinosaur skeletons, the CLDQ has received unrivaled attention in regards to taphonomic investigations and depositional interpretations over the last 85 years. The quarry was first formally excavated in 1926 (Miller and

others, 1996), though the first extensive work at the quarry did not begin until 1939, led by W.L. Stokes and a field crew from Princeton University (Stokes, 1945). From the 1960s through 2005 the quarry was worked intermittently by various field crews, most of which were based in Utah (e.g., Madsen 1976; Miller and others, 1996; Gates, 2005; Hunt and others, 2006). In 1968, the CLDQ was recognized as a U.S. Natural Landmark and is currently managed by the U.S. Bureau of Land Management (BLM), followed by the installation of two metal Butler buildings in the late 1970s (Miller and others, 1996). While the site receives frequent visitors and is a positive tourism spot for the state of Utah, the enigmatic nature of the fossil assemblage has produced numerous theories by the equally numerous taphonomic studies; this fact was noted by Madsen (1976, p. 8), who stated, “*Theories of the demise of the Cleveland-Lloyd dinosaurs are but slightly fewer in numbers than the visitors to the quarry.*”

Since its discovery in 1926, the CLDQ has yielded over 10,000 dinosaur bones (Gates, 2005). However, the various field expeditions that have excavated the quarry during that time have each established a different mapping method, many of which are not compatible with previous quarry maps. Whereas various depositional models have been proposed for the CLDQ, the lithologies, abundant vertebrate macrofossils, and rare microvertebrate and invertebrate remains suggest an ephemeral pond or similar overbank deposit with a fluctuating water table (calcareous mudstone facies) that became more permanently hydrated in the form of a shallow lacustrine setting (limestone facies) (Bilbey, 1999; Gates, 2005; Peterson and others, 2017). The presence of freshwater ostracods, gastropods, and charophytes in the limestone cap over the bone-bearing mudstone suggests that the environment supported a freshwater ecosystem during the last stages of sediment filling the pond (Bilbey, 1992). An ash bed approximately 1 m above the limestone cap has been dated to 147.2 ± 1 Ma to 146.8 ± 1 Ma via K/Ar dating (Bilbey, 1998).

METHODOLOGY

Field Excavation and Stabilization

Fieldwork was performed at the CLDQ between 2015 to 2017 by field crews from the University of

Wisconsin–Oshkosh and Indiana University of Pennsylvania. A total of 55 bones were mapped and photographed within the South Butler Building, representing bones exposed by previous expeditions and left exposed in the South Butler Building as well as newly exposed elements.

Grid Mapping

A grid map of the quarry was constructed using U.S. customary units, as this matches the data generated by the BLM previously (figure 2). Standard grid mapping of the South Butler Building was completed using a yard-by-yard PVC grid, containing 15 x 15 cm minor grid squares. Only data from the South Butler Building was used for this study, as the sample set available in the North Butler Building is skewed to bones at the base of the deposit. A 1-yard square grid frame constructed from PVC tubing and nylon cord on adjustable legs was aligned to a master grid line strung across the entire area of the quarry from fixed datums. This square was used to measure the position of bones within the larger master grid. Subsequently, the depth from an arbitrary fixed datum, the upper surface of the concrete foundation of the buildings, was measured via plumb bob at the ends of each bone, allowing for the calculation of dip and precise stratigraphic placement of each element. Field specimen numbers, including element field identifications and notes, were recorded according to the format established by prior crews; for example, CLDQ-001-17 was the first recorded specimen of 2017. Furthermore, the thickness of the undulating overlying limestone cap was measured in relation to the building foundation and bone position.

The resulting map presents the distribution of bones, with accompanying 3D orientation data (figures 2 and S1, table 1). Cardinal orientation was measured outside of the magnetic influence of the steel Butler Buildings (a likely reason for the cardinal inaccuracy of many maps drafted of the quarry after to the construction of the buildings in 1969) using a standard azimuthal compass-clinometer, adjusted for magnetic declination ($11^{\circ} 5' E$).

Subsequently, each bone element was plotted as a point in two cross sections along the long axis of the

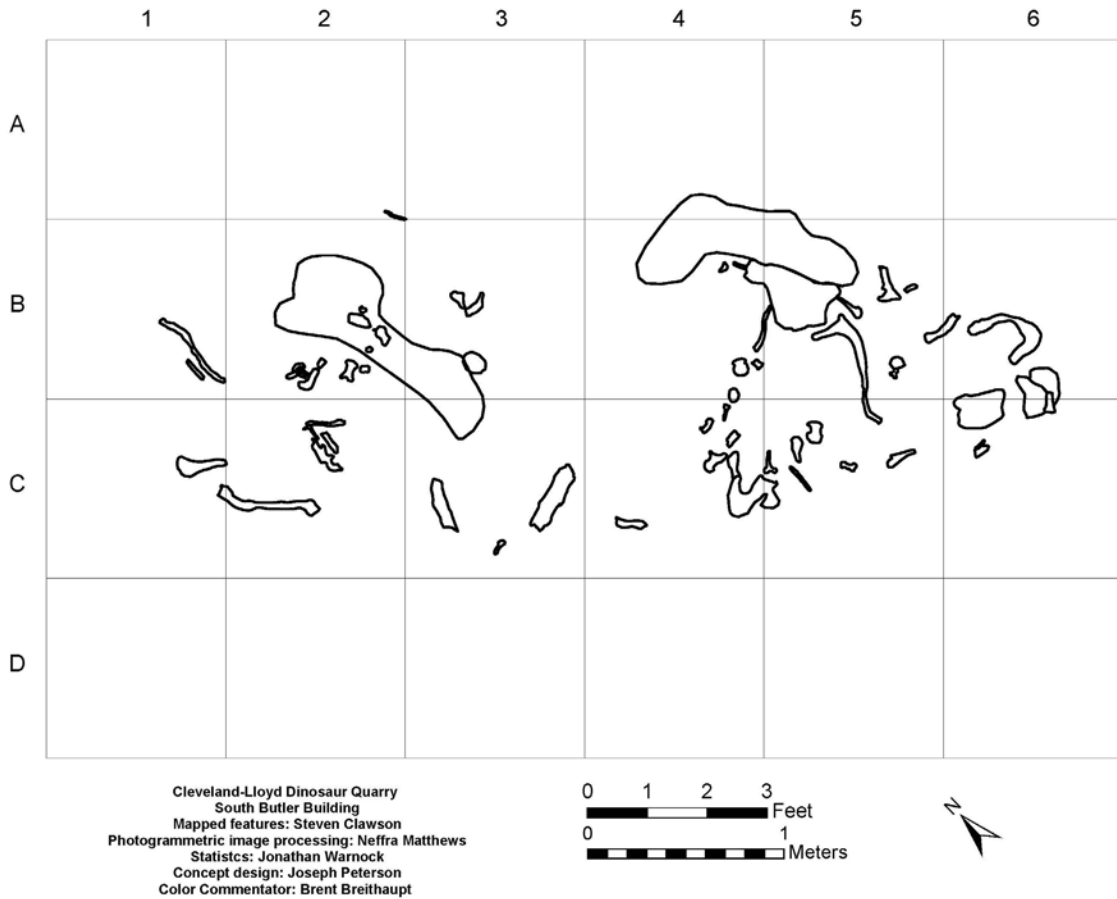


Figure 2. Standard grid map of the 2015–2017 excavations of the South Butler Building at the CLDQ.

South Butler building (35° west of north), utilizing depth and position data collected in the field. In addition to the bone position, the limestone thickness was plotted (figure 3). Two such cross sections were created in order to accommodate the lateral variability in limestone thickness, one through row B and one through row C of the master grid (figures 2 and 3). Rows A and D have not been plotted to date due to the small number of bones exposed in those grid rows.

Photogrammetry

Photographs were taken using a Nikon D3000 single-lens reflex (SLR) camera, maintaining an 18 mm focal length. Excluding a few skylights on the ceiling, quarry windows were covered with shades to minimize lighting effects. For the purposes of this photogram-

metric map, three rounds of photography were necessary: 90° (vertical, facing the quarry floor), 45° (intermediate, at an oblique angle with the quarry floor), and 0° (horizontal, facing the quarry wall), performed in a circular pattern around the inside of the building in two series: facing inward and facing outward. Four sets of photographic documentation took place; one in 2015 (547 photos), two collected in 2016 (436 and 446 photos), and one 2017 (404 photos). Calibrated photogrammetric targets were used during each photography session. Two methods were utilized when placing the targets. First, a series of targets were placed along the building's foundation at the location of the master grid lines. These targets served to align the grid map to the photogrammetric map. A second set of movable photogrammetric targets were placed within the excavation area and were repositioned between each photogram-

Table 1. Field specimen numbers and tentative field identifications are given for each bone in the South Butler Building. In addition, bone dimensions and positions are given. X = no data.

Field #	Field ID	Length (cm)	Width (cm)	Grid Square	Depth from Foundation (cm)	Limestone Thickness (cm)	Depth Below Limestone (cm)	Orientation with respect to North (°)
CLDQ-S-17-001	Rib	33	5	B1	121	31.75	74.25	175
CLDQ-S-17-002	Scap	128	48	B2-B3	122	29.21	77.79	14
CLDQ-S-17-003	Rib	13	2.5	B2	140.5	29.21	96.29	173
CLDQ-S-17-004	Toe	4	3	B2	119	29.21	74.79	20
CLDQ-S-17-005	Indet.	11	6	B2	111	29.21	66.79	20
CLDQ-S-17-006	Vertebra	11	10	B2	113	29.21	68.79	41
CLDQ-S-17-007	Toe	3.5	3	B2	113	29.21	68.79	6
CLDQ-S-17-008	Vertebra	15	14	B3	129	43.18	70.82	10
CLDQ-S-17-009	Vertebra	38	8	B3	123	43.18	64.82	X
CLDQ-S-17-010	Jacket	126	38	B4	94.5	49.53	29.97	X
CLDQ-S-17-011	Vertebra	56	32	B5	97.5	49.53	32.97	105
CLDQ-S-17-012	Rib	6.5	1.5	B4	102	49.53	37.47	35
CLDQ-S-17-013	Rib	24	3.5	B4	107.5	49.53	42.97	110
CLDQ-S-17-014	Centrum	9	8	B5	99.5	49.53	34.97	X
CLDQ-S-17-015	Rib	54	5.5	B5	100	38.35	46.65	160
CLDQ-S-17-016	Limb	18.5	5	B5	99	38.35	45.65	155
CLDQ-S-17-017	Rib	6.5	2.5	B5	100	38.35	46.65	35
CLDQ-S-17-018	Limb	14	6	B5	103	38.35	49.65	165
CLDQ-S-17-019	Limb	19	4	B5	98	38.35	44.65	90
CLDQ-S-17-020	Pelvic	37	20	B6	92	29.21	47.79	33
CLDQ-S-17-021	Femur	20	12	C6	98	58.42	24.58	155
CLDQ-S-17-022	Limb	26	17	C6	91	58.42	17.58	X
CLDQ-S-17-023	Indet.	24	18	C6	94	58.42	20.58	X
CLDQ-S-17-024	Rib	10	10	C6	92	58.42	18.58	73
CLDQ-S-17-025	Toe	5	2.5	C5	96	76.7	4.3	20
CLDQ-S-17-026	Meta	8	3	C5	106	76.7	14.3	43
CLDQ-S-17-027	Vertebra	12	12	C5	98	76.7	6.3	X
CLDQ-S-17-028	Ilium	50	24	C5	99	76.7	7.3	85
CLDQ-S-17-029	Rib	17	3	C5	96	76.7	4.3	155
CLDQ-S-17-030	Limb	X	X	C5	103	76.7	11.3	35
CLDQ-S-17-031	Cervical rib	10	3	C4	110	90	5	155
CLDQ-S-17-032	Quadrate	13	7	C4	112	90	7	155
CLDQ-S-17-033	Rib	9	5	C4	105	90	0	155
CLDQ-S-17-034	Indet.	12	8	C4	113	90	8	X
CLDQ-S-17-035	Centrum	10	7	C4	103	90	-2	X
CLDQ-S-17-036	Zygopophysis	10	2	C4	109	90	4	100
CLDQ-S-17-037	Vertebra	8	6	C4	107	90	2	X
CLDQ-S-17-038	Limb	11	3	C4	115	90	1	5
CLDQ-S-17-039	Femur (L)	36	10.5	C3	103	86.36	1.64	105
CLDQ-S-17-040	Surangular	27	8	C3	130	86.36	28.64	150
CLDQ-S-17-041	Vertebra	9.5	5.5	C2	115	58.42	41.58	85
CLDQ-S-17-042	Vertebra	6	3	C2	116	58.42	42.58	20
CLDQ-S-17-043	Dentary	12	7	C2	114	58.42	40.58	75
CLDQ-S-17-044	Atlas	10	2.5	C2	115	58.42	41.58	X
CLDQ-S-17-045	Limb	49	5	C2	99	58.42	25.58	15
CLDQ-S-17-046	Indet.	3	2	C2	115.5	58.42	42.08	160
CLDQ-S-17-047	Vertebra	30	8	C2	119	58.42	45.58	165
CLDQ-S-17-048	Superior process	9	5	C2	119	58.42	45.58	20
CLDQ-S-17-049	Trans process	20	2.5	C2	120	58.42	46.58	38
CLDQ-S-17-050	Humerus	23.5	7	C1	100	63.5	21.5	35
CLDQ-S-17-051	Limb	X	X	D3	102	86.36	0.64	180
CLDQ-S-17-052	Vertebra	19	17	C5	100	76.7	8.3	X
CLDQ-S-17-053	Gastralia	50	10	C6	135	0	120	180
CLDQ-S-17-054	Caudal vert	5	2	C6	98	58.42	24.58	75
CLDQ-S-17-055	Rib	100	60	C4	146	90	41	X

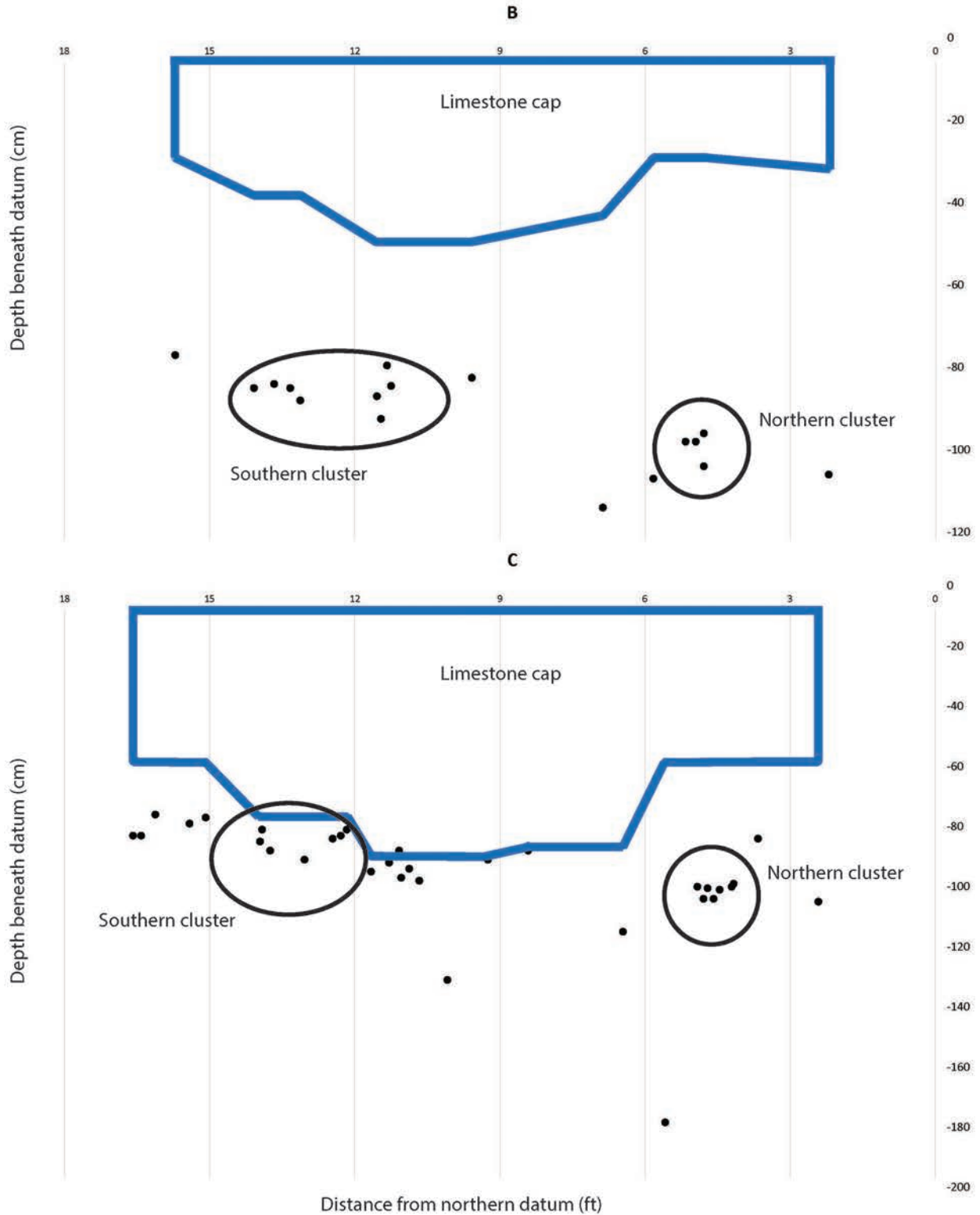


Figure 3. Cross sections through the bonebed. Cross sections are presented through the B and C rows of the grid map (figure 1). Black dots represent the centers of bones found in each row. Each cross section represents a two-dimensional compression of all of the bones found in each row. The thickness and undulatory lower surface of the limestone cap is shown. Following the convention of mapping previously done by the BLM the horizontal axis is measured in feet rather than meters.

metric session as new stratigraphic levels were exposed. All targets served to provide real world units to the photogrammetric processing. All 1833 digital photographs taken of the quarry were imported into Agisoft Photoscan Professional Edition, Version 1.3.2 Build 4205 (64 bit), an image-based 3D modeling/photogrammetric software package. Processing was conducted on a Dell Precision 7710 laptop with Intel Core i7 vPro processor, 32 GB of RAM, and an NVIDIA Quadro M5000M graphics card running Windows 10.

Software Procedure

To ensure uniformity among the episodes of photography all 1833 images were processed together in the same “chunk.” Agisoft Photoscan utilizes the term “chunk” to denote a grouping of images upon which the same structure from motion and alignment algorithms, as well as other processing functions, may be applied. The alignment was conducted with an accuracy setting of “High,” generic preselection was disabled so that all images were evaluated with each other for matches, key point limit was set to “80,000,” and tie-point limit was set to “0.” The time associated with this processing phase took 2 days and 21 hours for matching and 3 hours 23 minutes for alignment. The majority (97%) of images aligned successfully on high resulting in a sparse point cloud of over 7 million points. An error reduction and camera optimization workflow was followed (Matthews and others, 2016). Markers were placed along the upper surface of the concrete building foundation and cross beam at the master grid locations. The automatic coded target detection algorithm within Photoscan was

used to mark the calibrated photogrammetric targets and for assignment of scale bars of appropriate length. The units of the Photoscan project were set to meters. At the conclusion of the error reduction and optimization phase a reprojection error of 0.343 pixels was reached. Factoring in an average image resolution of 0.494 mm per pixel and a grid marker error of 0.495 mm a total photogrammetric project error of 1 mm was achieved. The “rotate object” tools was used within Photoscan to effectively level the upper surface of the building foundation without skewing or warping the aligned point cloud. The local dip of the CLDQ, estimated under 2° northwest in the Huntington 30' x 60' quadrangle (Witkind, 1988), was considered negligible for leveling. A user-defined coordinate system was chosen and an arbitrary elevation of 10 m set for the foundation to avoid negative elevations.

The chunk comprised of all episodes was duplicated multiple times to correspond to the four episodes of photographic documentation. Within each duplicate chunk one episode was chosen and the images from other episodes were disabled. Dense point clouds, meshes, a digital elevation model (DEM), and digital orthorectified image mosaics (orthomosaics) were generated for each episode chunk (table 2). The above procedure resulted in all of the photogrammetric products for each episode to be in a uniform coordinate system related to the quarry map grid system.

The orthomosaics and DEM for each episode were brought into ArcMAP 10.4.1 and polygons were drawn for each bone element and labeled according to the quarry map (figure 4). All statistics gathered during the excavation were recorded in a spreadsheet that was

Table 2. Statistics for four photogrammetry episodes from 2015–2017, including number of points in each dense point cloud, number of faces in each mesh after decimation, resolution of each DEM, and resolution of each orthomosaic image. Note: decimation of the meshes to 50 million (50,000,000) was necessary to ensure response computer processing.

Episode	Number of Points in Dense Point Cloud	Number of Faces in Mesh
May 2017	66,967,408 (high quality)	49,848,948
June 27, 2016	54,458,463 (high quality)	49,866,034
June 23, 2016	63,239,516 (high quality)	49,922,374
June 2015	66,241,247 (high quality)	49,999,022

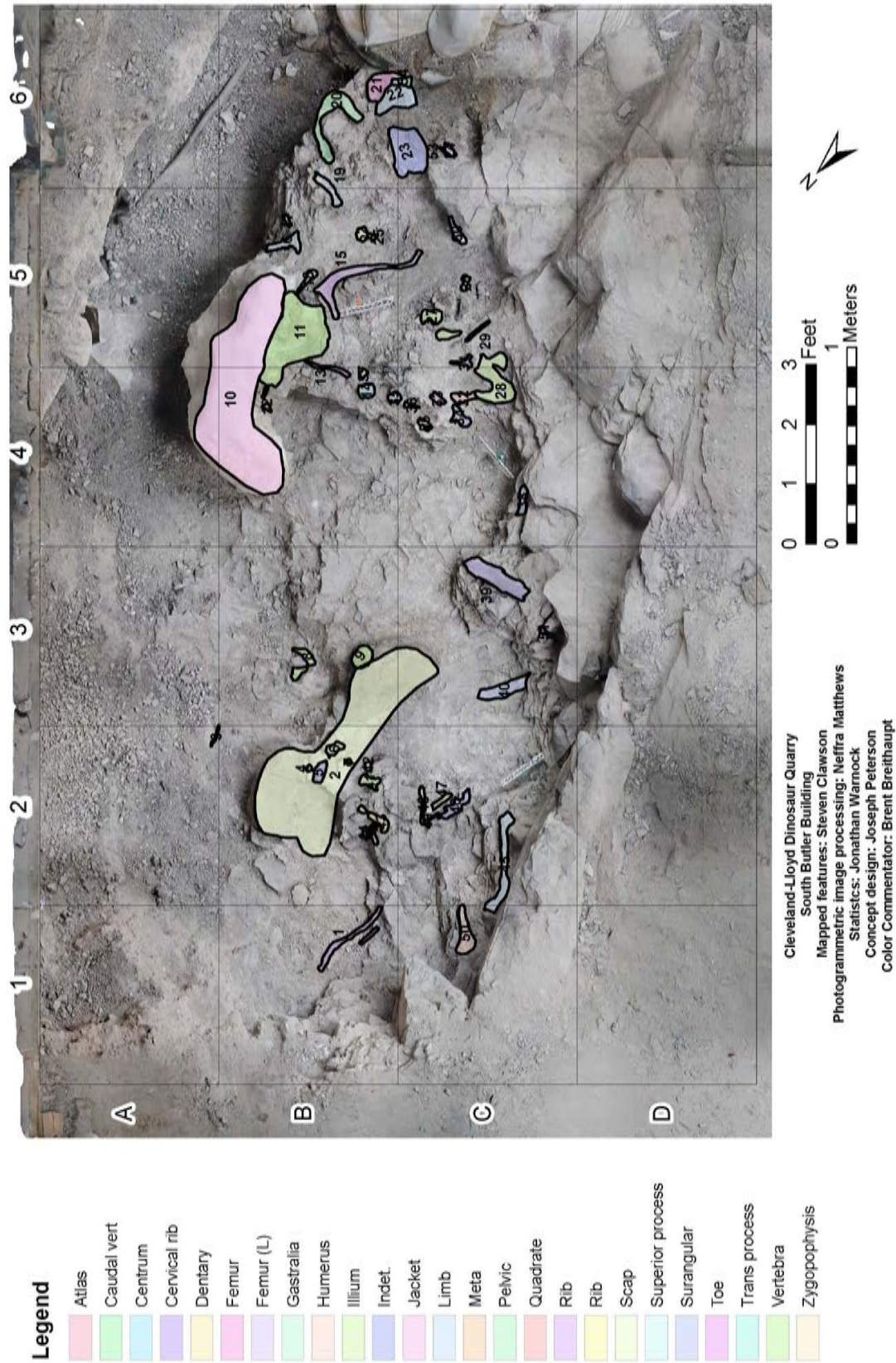


Figure 4. Orthomosaic map of the 2015–2017 excavations of the South Butler Building at the Cleveland-Lloyd Dinosaur Quarry produced from photogrammetry and standard grid mapping (figure 1). Field numbers correspond to bones designations listed in table 1. An interactive PDF (figure S1) is located in the attachment panel.

joined to the digital quarry map. This allows for visualization of the quarry, in 3D space, based on multiple combination of factors (supplemental figure S1). Figure S1 is an interactive photogrammetric model of the excavation in the South Butler Building at end of the 2017 field season that can be launched by clicking on figure S1 in the attachment panel. Activation of the Object Data Tool (Adobe) launches the interactive content, permitting selection of individual elements and browsing of element within the map, field number, measurements, depth data, and orientation. For bone designations refer to table 1.

Statistical Analysis

Circular means and Raleigh's R test for two data subsets were calculated using PAST (Hammer and others, 2001). The data was separated into two bins to calculate circular means based on a gap in bone deposition along a north/south transect. The first mean is calculated for bones found between 0 and 2.13 m (0 and 7 ft) from the north edge of the foundation of the South Butler Building (n = 19 bones) and the second mean represents bones found between 3.05 and 5.49 m (10 and 18 ft) from the north edge of the foundation (n = 29 bones). As above, feet were used rather than meters to insure continuity with the original grid set up by the Utah BLM. Three bones found between 2.13 and 3.05 m (7 and 10 ft) from the foundation were not included in the statistical analysis. Raleigh's R test was used to determine the the significance of the two circular means ($p < 0.05$). Finally, PAST was used to test for a significant ($p < 0.05$) difference in mean depth between the two bone clusters described above.

RESULTS

Bone depth and orientation data are provided in table 1. Bone orientations ranged from 0 to 175° from north. The limestone thickness varied from 29 to 90 cm and was found to vary in both the north-south and east-west directions. Bones were found from the limestone/siltstone contact to the base of current excavation.

Photogrammetry produced a 3D model of the quarry (figure 3) which can also act as a realistic true to scale map view of the quarry. In addition, photogrammetric

models produced throughout the course of excavation allow for the display of progressive excavation through the quarry (supplemental figure S2). Figure S2 is a "living map" of excavations. Animation showing the progression of excavation over the course of the 2015–2017 field seasons. Subsequent rounds of photogrammetry can be added as field work continues, providing a visual means to assess the distribution and relative positions of bones even after they are removed from the quarry. The animation can be activated by clicking on figure S2 in the attachment panel. All photogrammetric products are to scale and provide a detailed view of the excavation.

Two distinct clusters of bone were observed during excavation. The northernmost bone cluster was found to have an average orientation of 60.3° whereas the southernmost bone cluster has an average orientation of 101°. Both of these means were found to be significant. In addition, the north bone cluster has an average depth of 119 cm beneath the foundation of the South Butler Building, whereas the south bone cluster has an average depth of 102 cm. These means were found to be significantly different.

DISCUSSION

A robust orientation analysis is necessary to interpret the paleoenvironment of a bonebed (e.g., Voorhies, 1969; Behrensmeyer, 1975; Rogers and Kidwell, 2007; Mathews and others, 2009; Keenan and Scannella, 2014). The photogrammetric scalar field mesh produced by this study offers a 3D alternative to 2D projections for interpreting orientations. By collecting photogrammetric data over the course of many field seasons, a "living" map can be generated (figure S2). This map allows for researchers to view individual bone horizons in three dimensions at multiple excavation levels and can be updated as frequently as new pictures are taken during excavation. By viewing subsequent years of photogrammetry, the placement of bones which have been removed can be compared to those still in place, allowing for detailed previously impossible visualization of the quarry assemblage in a stratigraphic context. Furthermore, photogrammetric maps can ground-truth field maps and orientation data collected during exca-

vation. The currently produced photogrammetric map includes embedded data for depth, size, orientation, and field identification of each bone element.

The creation of a 'living' map, in which multiple stratigraphic horizons may be viewed by accessing data across multiple years of photogrammetry, is a novel feature in vertebrate paleontology. Combining the aforementioned mapping techniques with photogrammetry reveals multiple depositional bone-bearing layers separated by bone-free horizons. This new technique suggests the genesis of the assemblage could be owed to multiple overlapping depositional events. Additionally, abiotic taphonomic signals apparent in the photogrammetric map, e.g., clustering of bone, preferred orientations and preferred depths, support the hypothesis that the CLDQ represents an ephemeral pond system periodically flooded with overbank sediments (*sensu* Peterson and others, 2017). This new technique, one that can be continually updated by subsequent expeditions and hopefully any subsequent research groups, will help institute a system for the collection of more precise bone orientation data at the CLDQ.

The data presented here represent the first 3D bone distribution data published on the CLDQ since excavation began in 1926. Based on 3D analysis of bone position and orientation via field maps, photogrammetric maps and cross sections, the bones currently exposed in the South Butler Building can be separated into two main clusters and several isolated elements. The clusters are distinct in that they are physically separated into a northern and southern group. Furthermore, each cluster has a distinct and statistically significant orientation. Additionally, whereas there is some stratigraphic overlap, the northern bone group has a deeper average depth than the southern bone group relative to a fixed datum and the mean depths of each cluster are significantly different. It is worth noting that only a small area of the quarry has been mapped in such a way to provide this detailed 3D analysis. The results found here may or may not reflect conditions within the entire bonebed. Future excavation will provide the opportunity to check these results against other sections of the bonebed.

Also striking is that the lateral extent of each cluster of bones is constrained by a single large bone and each cluster is composed of associated skeletal remains, al-

though it is currently impossible to be certain the associated elements are from a single individual. The northern cluster of bones is primarily composed of associated *Allosaurus* skull elements as well as small vertebrae and associated pedal elements. These bones are clustered against the medial surface of a large (146 cm length) sauropod left scapula. The southern cluster is comprised mainly of disarticulated and associated vertebrae and disarticulated ribs which are clustered against two articulated sauropod cervical vertebrae (63 cm total length). In both cases the large bone elements (scapula, articulated vertebrae) create a surface against which the smaller bone elements came to rest. Furthermore, in both cases the smaller bones resting against the larger elements are associated skeletal elements. This data very strongly supports a bloat and float taphonomic scenario in those areas of the quarry studied and described herein. It is compelling to think about the scenario being present for the entire quarry, but because 3D data is not available for most the quarry area, this interpretation can only be speculated upon for the remainder of the bonebed. However, further work may provide additional evidence in this regard.

This evidence suggests that bloat and float processes were important to the formation of the CLDQ deposits. Bloat and float is a process which distributes bones from decaying corpses (e.g., Syme and Salisbury, 2014). During the early stages of decomposition, corpses bloat. This makes them buoyant and causes them to float. As the bodies continue to decay, segments of the body (i.e., a limb, head, or section of the vertebral column) fall off and rot further. As such, bloat and float processes should result in an accumulation of randomly scattered groupings of associated and articulated bone. If a strong current is present during the bloat and float process, these bones may accumulate against the surface of the depositional basin or fall and settle with a preferred orientation. It is worth noting, however, that bloat and float processes can lead to the deposition of whole skeletons as well (e.g., Mallon and others, 2018).

Bloat and float within the pond setting represented by the CLDQ deposit would result in bones being associated as they distribute. This setting is influenced by both fluvial (e.g., deposition of sediments escaping the riverbed during high flow periods) and paludal (e.g.,

settling and weak wind-induced wave action) processes. We hypothesize that a weak current within the pond (e.g., short-term flow induced by wind blowing across the pond surface) would have moved rotting carcasses as they fell through the water column, occasionally resting against larger previously deposited skeletal remains which had already sunk to the pond floor. For example, a partially decomposing *Allosaurus* skull may float into pond during a flood stage. During further decomposition, the skull would disarticulate and begin falling through the water column. While falling, elongated elements would orient parallel to any weak current, and settle against a large sauropod scapula and previously deposited vertebrae and pedal elements. These bones are then buried together, maintaining the orientation at depth. Those bones which did not come to rest against a larger element are represented by the isolated elements found within the quarry. It is also possible that desiccated remains could have been washed into the CLDQ pond and rapidly buried to produce the pattern of bone deposition seen here. However, this would require the remains to have been exposed for only a short amount of time, as no evidence of flaking from exposure to the sun is evident on the bones. Furthermore, an increased number of scavenging traces would be expected on remains sitting at the surface.

Past research at the CLDQ has suggested that the deposit may represent multiple depositional events (Peterson and others, 2017). The data presented here provide further evidence that multiple depositional events may have occurred to create the CLDQ bonebed. The two identified clusters of bone both have distinct, significant orientations. This implies at least two flow directions were involved in the depositional history of this section of the quarry. Additionally, the two bone clusters have distinct mean depths. Whereas there is some overlap in the depths represented by these clusters, this could be due to the uneven surface of the bottom of the pond at the time of each depositional event. Multiple depositional events controlled primarily by bloat and float processes would lead to the formation of an undulatory surface at the bottom of the pond, as isolated clusters of bones draped with mud would create local topographic highs. The undulation of the limestone layer provides evidence of an uneven surface to

the bottom of the pond, at least during the final phase of deposition. Burial after each depositional event must have been rapid, given that the bones are unabraded, nearly all lack vertebrate and insect scavenging marks, and lack evidence of physical weathering (Behrensmeier, 1975; Gates, 2005).

The spatial distribution of bone at the CLDQ is at odds with other Morrison Formation vertebrate localities. Bones at the Mygatt-Moore Quarry are found disarticulated and rarely associated (Kirkland and others, 2005) in an environment interpreted as a vernal pool on a poorly drained muddy floodplain, with abundant plant life, possibly from a surrounding woodland (Kirkland and others, 2005; Foster and Hunt-Foster, 2011; Foster and others, 2018). Hence, bone distribution data don't currently support bloat and float processes at Mygatt-Moore. Four additional sauropod-dominated bonebeds from the Brushy Basin Member of the Morrison Formation (the Howe Quarry near Shell, Wyoming, the BS and SI Quarries near Thermopolis, Wyoming, and the Carnegie Museum *Diplodocus* Quarry near Sheep Creek, Wyoming) have similar lithologies to the CLDQ (i.e., calcareous mudstone) and also display considerable disarticulation of skeletal remains (Michelis, 2004; Ikejiri and others, 2006; Jennings and Hasiotis, 2006; Brezinski and Kollar, 2008). All four sites are interpreted as low-energy, poorly drained floodplains associated with seasonal palustrine or lacustrine depositional environments similar to that observed in the CLDQ. However, the high frequency of shed theropod teeth in close proximity to sauropod remains at the SI Quarry suggest active feeding took place, disarticulating the skeletal elements by biostratinomic processes (Jennings and Hasiotis, 2006). Both the SI and BS sites are interpreted to represent single depositional events (Ikejiri and others, 2006; Jennings and Hasiotis, 2006) rather than cyclic processes (Peterson and others, 2017).

Despite differences with other Morrison Formation localities, similarities are evident between the CLDQ and smaller bonebeds that have been described from other formations. Fiorillo and others (2000) described a *Placerias* bonebed from the Upper Triassic Chinle Formation that is interpreted as a low-energy environment that also possesses numerous carbonate nodules that are pedogenic in origin. Bones also pos-

sess minimal evidence of fluvial transport, trampling, or predation (Fiorillo and others, 2000). Keenan and Scannella (2014) described a *Triceratops* bonebed from the Upper Cretaceous Hell Creek Formation (Garfield County, Montana). Whereas the bones of multiple *Triceratops* individuals were recovered in association (MNI = 3), differences among the abrasion and orientations of bones belonging to each individual suggest that aggregation of each carcass occurred through the force of multiple independent flooding events (Keenan and Scannella, 2014). The majority of bones at this bonebed are well preserved, showing little weathering and abrasion or biostratinomic alteration providing further similarity to those of the CLDQ. Additionally, many of these bones are “stacked,” as observed in the clustered bones at the CLDQ. Unlike the CLDQ, the *Triceratops* bones are positioned in layers of clay-rich siltstone associated with some microvertebrate remains (e.g., gar scales) (Keenan and Scannella, 2014) implying differences in the freshwater environments represented by each site. Regardless, the similarity of orientation and stacking imply similar depositional processes, i.e., multiple depositional events.

A similar mode of genesis is evident in a second *Triceratops* bonebed recovered from the upper Hell Creek Formation in Carter County, Montana (the “Homer” locality) (Matthews and others, 2009). The bone-bearing layer is roughly 0.5 m thick, and comprises bones that show little to no abrasion, with some small, heavily abraded elements likely representing a background accumulation as a function of its position in a floodplain (Matthews and others, 2009). Furthermore, these remains exhibit the same stacking pattern and are in some cases clustered against 2-m-long fossilized logs. This deposit represents only a single depositional event; however, bloat and float processes are likely given the association of elements. Similarities in the 3D clustering of bones at the CLDQ and the “Homer” locality support similar attritional processes, bloat and float, were significant at both sites.

CONCLUSION

The maps and data presented here are significant in that they represent the first 3D data published on the

distribution of bones from the CLDQ. Adding the vertical perspective to analysis of bone deposition allows for refined understanding of depositional processes. Based on bone orientation and clustering patterns, we hypothesize that bloat and float processes have led to the distribution of bones found within the quarry. This can be seen in the common association, but rare articulation, of elements at the CLDQ. Additionally, bloat and float mechanisms would explain the clustering of numerous small associated bones against larger bones. Intriguingly, the spatial distribution of bones seen here suggests the possibility of multiple depositional events. If confirmed, the presence of multiple depositional layers may have profound impacts on the understanding of *Allosaurus* ecology. Regardless, 3D mapping techniques have added to the understanding of taphonomic processes controlling the CLDQ.

ACKNOWLEDGMENTS

We thank Michael Leschin, ReBecca Hunt-Foster, and Greg McDonald of the Utah Office of the BLM for facilitating fieldwork and processing permits. All fieldwork was conducted under permit number UT12-003E. Financial support was provided by the University of Wisconsin–Oshkosh Faculty Development Fund (Grant #FDM250) and by the Utah Office of the BLM. Thanks to formal reviewers Stuart Pond (Stuart Pond Design Ltd.) and Matteo Belvedere (Section D’archéologie et Paléontologie, Porrentruy, Switzerland), as well as James I. Kirkland (Utah Geological Survey) and Peter L. Falkingham (Liverpool John Moores University), for reviewing the manuscript and offering constructive feedback. We also thank Richard G. Clawson for field and laboratory support during the 2012–2017 field seasons. Finally, we offer special thanks to the numerous volunteer field crews from the 2013 and 2017 field seasons.

REFERENCES

- Behrensmeyer, A.K., 1975, The taphonomy and paleoecology of Plio-Pleistocene vertebrate assemblages east of Lake Rudolf, Kenya: *Bulletin of the Museum of Comparative Zoology*, v. 145, no. 10, p. 473–574.
- Bilbey, S.A., 1992, Stratigraphy and sedimentary petrology of the

- Upper Jurassic-Lower Cretaceous rocks at Cleveland-Lloyd Dinosaur Quarry with a comparison to the Dinosaur National Monument Quarry: Salt Lake City, University of Utah, Ph.D. dissertation, 295 p.
- Bilbey, S.A., 1998, Cleveland-Lloyd Dinosaur quarry age, stratigraphy and depositional environments, in Carpenter K., Chure D., and Kirkland J.I., editors, *The Morrison Formation—an interdisciplinary study: Modern Geology*, v. 23, p. 87–120.
- Bilbey, S.A., 1999, Taphonomy of the Cleveland-Lloyd Dinosaur Quarry in the Morrison Formation, central Utah—a lethal spring-fed pond, in Gillette, D.D., editor, *Vertebrate paleontology in Utah: Utah Geological Survey Miscellaneous Publication 99-1*, p. 121–134.
- Breithaupt, B.H., Matthews, N.A., and Noble, T.A., 2004, An integrated approach to three-dimensional data collection at dinosaur tracksites in the Rocky Mountain West: *Ichnos*, v. 11, no. 1–2, p. 11–26.
- Brezinski, D.K., and Kollar, A.D., 2008, Geology of the Carnegie Museum dinosaur quarry site of *Diplodocus carnegii*, Sheep Creek, Wyoming: *Annals of Carnegie Museum*, v. 77, no. 2, p. 243–252.
- Carpenter, K., 2010, Variation in a population of Theropoda (Dinosauria)—*Allosaurus* from the Cleveland-Lloyd Quarry (Upper Jurassic), Utah, USA: *Paleontological Research*, v. 14, no. 4, p. 250–259.
- Dodson, P., Behrensmeyer, A.K., Bakker, R.T., and McIntosh, S.J., 1980, Taphonomy and paleoecology of the dinosaur beds of the Jurassic Morrison Formation: *Paleobiology*, v. 6, p. 208–232.
- Engelmann, G.F., Chure, D.J., and Fiorillo, A.R., 2004, The implications of a dry climate for the paleoecology of the fauna of the Upper Jurassic Morrison Formation: *Sedimentary Geology*, v. 167, p. 297–308.
- Falkingham, P.L., 2012, Acquisition of high-resolution three-dimensional models using free, open-source, photogrammetric software: *Palaeontologica Electronica*, v. 15, no. 1, p. 1–15.
- Fiorillo, A.R., Padian, K., and Musikasinthorn, C., 2000, Taphonomy and depositional setting of the *Placerias* Quarry (Chinle Formation: Late Triassic, Arizona): *Palaios*, v. 15, no. 5, p. 373–386.
- Foster, J.R., and Hunt-Foster, R.K., 2011, New occurrences of dinosaur skin of two types (Sauropoda? and Dinosauria indet.) from the Late Jurassic of North America (Mygatt-Moore Quarry, Morrison Formation): *Journal of Vertebrate Paleontology*, v. 31, no. 3, p. 717–721.
- Foster, J.R., and Peterson, J.E., 2016, First report of *Apatosaurus* (Diplodocidae: Apatosaurinae) from the Cleveland-Lloyd Dinosaur Quarry in the Upper Jurassic Morrison Formation of Utah—abundance, distribution, paleoecology, and taphonomy of an endemic North American sauropod clade: *Palaeoworld*, v. 25, no. 3, p. 431–443.
- Foster, J.R., Hunt-Foster, R.K., Gorman M.A., II, Trujillo, K.C., Suarez, C.A., McHugh, J.B., Peterson, J.E., Warnock, J.P., and Schoenstein, H.E., 2018, Paleontology, taphonomy, and sedimentology of the Mygatt-Moore Quarry, a large dinosaur bonebed in the Morrison Formation, western Colorado—implications for Upper Jurassic dinosaur preservation modes: *Geology of the Intermountain West*, v. 5, p. 23–93.
- Gates, T.A., 2005, The Late Jurassic Cleveland-Lloyd Dinosaur Quarry as a drought-induced assemblage: *Palaios*, v. 20, p. 363–375.
- Gilmore, C.W., 1920, Osteology of the carnivorous dinosauria in the United States National Museum, with special reference to the genera *Antrodemus* (*Allosaurus*) and *Ceratosaurus*: *Bulletin of the United States National Museum*, v. 110, p. 1–154.
- Hammer, Ø., Harper, D.A.T., and Ryan, P.D., 2001, PAST—Paleontological statistics software package for education and data analysis: *Palaeontologica Electronica*, v. 4, no. 1, 9 p.
- Hanna, R.R., 2002, Multiple injury and infection in a sub-adult theropod dinosaur *Allosaurus fragilis* with comparisons to allosaur pathology in the Cleveland-Lloyd Dinosaur Quarry collection: *Journal of Vertebrate Paleontology*, v. 22, no. 1, p. 76–90.
- Hunt, A.P., Lucas, S.G., Krainer, C., and Spielmann, J., 2006, The taphonomy of the Cleveland-Lloyd Dinosaur Quarry, Upper Jurassic Morrison Formation, Utah—a re-evaluation, in Foster, J.R., and Lucas, S.G., editors, *Paleontology and geology of the Upper Jurassic Morrison Formation: New Mexico Museum of Natural History and Science Bulletin 36*, p. 57–67.
- Ikejiri, T., Watkins, P., and Gray, D., 2006, Stratigraphy, sedimentology, and taphonomy of a sauropod quarry from the upper Morrison Formation of Thermopolis, central Wyoming, in Foster, J.R., and Lucas, S.G., editors, *Paleontology and geology of the Upper Jurassic Morrison Formation: New Mexico Museum of Natural History and Science Bulletin 36*, p. 39–46.
- Jennings, D.S., and Hasiotis, S.T., 2006, Taphonomic analysis of a dinosaur feeding site using geographic information systems (GIS), Morrison Formation, southern Bighorn Basin, Wyoming, USA: *Palaios*, v. 21, no. 5, p. 480–492.
- Keenan, S.W., and Scannella, J.B., 2014, Paleobiological implications of a *Triceratops* bonebed from the Hell Creek Formation, Garfield County, northeastern Montana: *Geological Society of America Special Paper 503*, p. 349–364.
- Kirkland, J.I., Scheetz, R.D., and Foster, J.R., 2005, Jurassic and Lower Cretaceous dinosaur quarries of western Colorado and eastern Utah, in Rishard, G., compiler, *Rocky Mountain Section of the Geological Society of America Field Trip Guidebook: Grand Junction Geological Society Field Trip 402*, p. 1–26.

- Madsen, J.H., Jr., 1976, *Allosaurus fragilis*—a revised osteology: Utah Geological Survey Bulletin 109, p. 1–163.
- Mallon, J.C., Henderson, D.M., McDonough, C.M., and Loughry, W.J., 2018, A “bloat-and-float” taphonomic model best explains the upside-down preservation of ankylosaurs: *Palaeogeography, Palaeoclimatology, and Palaeoecology*, v. 497, p. 117–127.
- Matthews, N.A., 2008, Aerial and close-range photogrammetric technology—providing resource documentation, interpretation, and preservation: Technical Note, U.S. Department of the Interior, Bureau of Land Management, National Operations Center, Denver, Colorado, v. 428, p. 1–42.
- Mathews, J.C., Brusatte, S.L., Williams, S.A., and Henderson, M.D., 2009, The first *Triceratops* bonebed and its implications for gregarious behavior: *Journal of Vertebrate Paleontology*, v. 29, no. 1, p. 286–290.
- Matthews, N.A., Noble, T.A., and Breithaupt, B.H., 2016, Close-range photogrammetry for 3D ichnology—the basics of photogrammetric ichnology, in Falkingham, P.L., Marty, D. and Richter, A., editors, *Dinosaur tracks—next steps*: Bloomington, Indiana University Press, 520 p.
- Michelis, I., 2004, *Taphonomie des Howe Quarry’s (Morrison-Formation, Oberer Jura)*, Bighorn County, Wyoming, USA: Bonn, Germany, University of Bonn, Ph.D. dissertation, 82 p.
- Miller, W.E., Horrocks, R.D., and Madsen, J.H., Jr., 1996, The Cleveland-Lloyd Dinosaur Quarry, Emery County, Utah—a U.S. National Landmark (including history and quarry map): *Brigham Young University Geology Studies*, v. 41, p. 3–24.
- Peterson, J.E., Warnock, J.P., Eberhart, S.L., Clawson, S.R., and Noto, C.R., 2017, New data towards the development of a comprehensive taphonomic framework for the Late Jurassic Cleveland-Lloyd Dinosaur Quarry, central Utah: *PeerJ*, doi: 10.7717/peerj.3368
- Richmond, D.R., and Morris, R.K., 1996, The dinosaur death-trap of the Cleveland-Lloyd Quarry, Emery County, Utah, in Moralis, M., editor, *The continental Jurassic: Museum of Northern Arizona Bulletin* 60, p. 533–545.
- Rogers, R.R., and Kidwell, S.M., 2007, A conceptual framework for the genesis and analysis of vertebrate skeletal concentrations, in Rogers, R.R., Eberth, D.A., and Fiorillo, A.R., editors, *Bonebeds—genesis, analysis, and paleobiological significance*: Chicago, Illinois, University of Chicago Press, p. 1–64.
- Syme, C.E., and Salisbury, S.W., 2014, Patterns of aquatic decay and disarticulation in juvenile Indo-Pacific crocodiles (*Crocodylus porosus*), and implications for the taphonomic interpretation of fossil crocodyliform material: *Palaeogeography, Palaeoclimatology, Palaeoecology*, v. 412, p. 108–123.
- Stokes, W.L., 1945, A new quarry for Jurassic dinosaurs: *Science*, v. 101, p. 115–117.
- Stokes, W.L., 1985, *The Cleveland-Lloyd Dinosaur Quarry—window to the past*: U.S. Department of the Interior, Bureau of Land Management, U.S. Government Printing Office, 61 p.
- Suarez, M.B., 2003, *Analysis of freshwater limestones at the Cleveland-Lloyd Dinosaur Quarry, Emery County, Utah*: San Antonio, Texas, Trinity University Department of Geosciences, senior thesis, 63 p.
- Voorhies, M.R., 1969, *Taphonomy and population dynamics of an early Pliocene vertebrate fauna, Knox County, Nebraska: Contributions to Geology*, University of Wyoming, Special Paper v. 1, p. 1–69.
- Witkind, I.J., compiler, 1988, *Geologic map of the Huntington 30' x 60' quadrangle, Carbon, Emery, Grand, and Uintah Counties, Utah*: U.S. Geological Survey Miscellaneous Investigations Series Map I-1764, 1 plate, scale 1:100,000.

